iMRI 2024;28(1);36-42
https://doi.org/10.13104/imri.2024.0005
eISSN 2384-1109

Original Article

Received: February 14, 2024
Revised: February 28, 2024
Accepted: March 4, 2024

Correspondence
Young Han Lee, MD, PhD
Department of Radiology, Research Institute of Radiological Science, and Center for Clinical Imaging Data Science (CCIDS), Yonsei University College of Medicine, 50-1 Yonsei-ro, Seodaemun-gu, Seoul 03722, Korea.
E-mail: sando@yuhs.ac

Fast Imaging of Shoulder MR Arthrography With Compressed Sensing Accelerated Isovolumetric 3D-THRIVE Sequence: Comparing One Isovolumetric Scan With Multiplanar Reconstruction and Three Conventional MR Images

Youngho Won, Jiwoo Park, Joohee Lee, Ho-Taek Song, and Young Han Lee

Department of Radiology, Research Institute of Radiological Science, and Center for Clinical Imaging Data Science (CCIDS), Yonsei University College of Medicine, Seoul, Korea

Purpose: This study compared 3D-T1 high resolution isovolumetric examination (3D-THRIVE) multiplanar reconstruction (MPR) imaging of shoulder magnetic resonance arthrography (MRA) with conventional MR images and validated the diagnostic agreements of isovolumetric MRA with and without compressed sensing (CS).
Materials and Methods: Seventy-three patients who underwent shoulder MRA, including image sets of conventional 2D fast spin echo (FSE) sequences and isotropic 3D-THRIVE sequences with and without CS, were evaluated. The CS acceleration factor was set to 1.5. In the first session, MPR images on the 3D-THRIVE sequence with CS were analyzed using current standard 2D FSE sequences in the axial, oblique-coronal, and oblique-sagittal planes. In the second session, 3D-THRIVE sequences with and without CS were compared with respect to image quality and degree of artifacts. Overall image quality scores and artifacts for conventional 2D images and 3D-THRIVE MPR with CS were analyzed using a paired t-test. The diagnostic agreement for pathological lesions of the shoulder in 3D-THRIVE with and without CS was evaluated using intraclass correlation coefficients.
Results: CS in the isotropic 3D-THRIVE showed a reduction in scanning time from 104 s (non-CS) to 81 s (CS). The diagnostic agreement between 2D FSE and 3D-THRIVE for shoulder tendon pathologies was excellent for subscapularis, supraspinatus, infraspinatus, and biceps tendons. The inter-rater agreements were excellent, and CS-3D-THRIVE demonstrated excellent diagnostic agreement for certain tendon pathologies compared with 3D-THRIVE without CS.
Conclusion: CS-accelerated isotropic 3D-THRIVE shoulder MRA can provide diagnostically acceptable images of tendon pathology with a reduced scan time. Shoulder MRI using 3D-THRIVE with CS may replace standard 2D FSE sequences in patients who require rapid imaging.

Keywords: Magnetic resonance imaging; Musculoskeletal; Compressed sensing

INTRODUCTION

Rotator cuff and labral abnormalities are common in patients with shoulder pain. Common diagnostic imaging modalities for shoulder-related diseases include magnetic resonance imaging (MRI), magnetic resonance arthrography (MRA), and multidetector computational tomography arthrography. Among these modalities, MRI of the shoulder joint is the most frequently used for detecting rotator cuff and labral abnormalities because of its high sensitivity and specificity [1-3]. Nevertheless, the use of conventional MRI for shoulder diagnosis remains controversial when considering which technique in MR sequences should be used in terms of accuracy, cost-effectiveness, and minimally invasive approach to intra-articular injection. Shoulder MRA is a well-known imaging technique with shoulder joint distension that enables optimization of soft tissue contrast. MRA has proven to be more sensitive in detecting rotator cuff and labral abnormalities [4,5]. Because conventional shoulder MRA requires at least three planes, the total scan time for a patient is inevitably long. In addition, intra-articular injection of contrast media causes patient anxiety, discomfort, and pain [6,7], which can result in motion artifacts during MRI scans [8]. Recently, fast MRI has accelerated in parallel with the application of compressed sensing (CS) to improve patient engagement and time efficiency as one of methods to reduce the scan time of MRI.

Three-dimensional (3D) isotropic MR sequences offer the advantages of fewer partial volume effects and provide consecutive images with thinner slices. This can maximize soft tissue contrast [9] and help in the diagnosis of shoulder pathology [10]. However, 3D imaging has several limitations. The time required to acquire images using 3D MR sequences is relatively long, which can result in patient discomfort, pain, and unwanted movements. Moreover, MRI scanning under suboptimal conditions may yield inferior and blurry images. To reduce the acquisition time, MRI acceleration methods including parallel imaging and CS have been investigated [11-15].

CS technology is based on undersampling, which means that the k-space is not completely filled [16,17]. Recently, the application of CS in 3D-fast spin echo (FSE) imaging of the shoulder joint was introduced. Consequently, the scanning time has decreased [18]. As no studies have focused on the application of CS to musculoskeletal imaging using 3D-T1 high resolution isovolumetric examination (3D-THRIVE) sequences with multiplanar reconstruction (MPR) capability, this study aimed to compare 3D-THRIVE imaging with and without CS for shoulder MRA, and to evaluate image quality as well as diagnostic agreements.

MATERIALS AND METHODS

Study Population

This retrospective study was approved by our institutional review board (IRB 4-2024-0010). The IRB waived the requirement for informed consent owing to the retrospective nature of the study. Shoulder MRA images in a clinical study were obtained from 97 patients with shoulder pain who underwent shoulder MRA in isotropic 3D-THRIVE sequences without and with CS between September 2017 and August 2018. Twenty-four patients who lacked CS-3D-THRIVE MRI data or presented scheduling constraints in the MRI imaging suite were excluded. The remaining study population comprised of 38 men (aged 21–78 years; mean age, 55.8 years) and 35 women (aged 30–81 years; mean age, 62.6 years), and were taken by the 3D-THRIVE sequence with respect to the axial plane to the patients related to the shoulder diseases (Fig. 1).

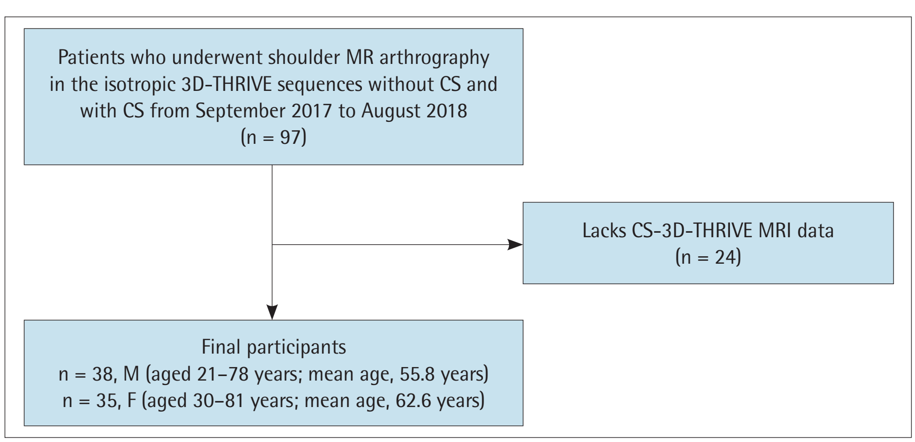

Fig. 1. Inclusion and exclusion flowchart of the study. Of the 97 patients who underwent shoulder MR arthrography from September, 2017 to August, 2018, 24 patients who lacked CS-3D-THRIVE MRI data were excluded and the remaining 73 patients were included in the study. MR, magnetic resonance; 3D-THRIVE, 3D-T1 high resolution isovolumetric examination; CS, compressed sensing; MRI, magnetic resonance imaging.

Intra-Articular Injection

All the patients received an intra-articular injection of 15–18 mL of diluted gadoterate meglumine solution with a concentration of 0.08 mL of Dotarem® (Guerbet, Villepinte, France) per 18 mL of normal saline and 2 mL of iodine contrast into the glenohumeral joint to be performed by fluoroscopic guidance before the scan of MRA. All MRI examinations were performed on a 3-T MR system (Ingenia CX®, Philips Healthcare, Best, The Netherlands) with a dedicated 16-channel sensitivity encoding (SENSE) shoulder coil (Philips Shoulder coil, Philips Healthcare). Patients were setup in the supine position with their arms in a neutral position.

Imaging Protocol on the Isovolumetric 3D-THRIVE Sequence MRA

After the intra-articular injection, 73 patients underwent the 3D-THRIVE sequence MRA without CS. The images obtained included conventional fat-suppressed T2-weighted FSE images of the axial, oblique sagittal, and oblique coronal planes; 3D-THRIVE sequences; and CS-3D-THRIVE sequences. When the conventional shoulder MRA imaging was applied to a patient with shoulder pain, imaging protocol for the 3D-THRIVE was repetition time (TR)/echo time (TE) = 6.9844/3.443 ms; flip angle 10°; 1.2 mm slice thickness and 0.6 mm slice overlap; field of view 120 × 120 mm; acquisition matrix 208 × 207; and number of acquisitions, 1. When CS acceleration was used in parallel with conventional shoulder MRA, the CS acceleration factor was 1.5. The MRI parameters for the T1 sequence on 3D-THRIVE were the same as the MR parameters. The details of the MR protocol are shown in Table 1.

Image Analysis

In the first session, MPR images were evaluated on the 3D-THRIVE sequence using the current standard 2D FSE sequences in the axial, oblique-coronal, and oblique-sagittal planes. All three planes of 2D FSE images were simultaneously reviewed by the reviewers. The axial THRIVE sequences and the reformatted sagittal and coronal images were reviewed by the reviewers. Diagnostic agreements were evaluated for pathological lesions of the supraspinatus, subscapularis, and biceps tendons between the 2D FSE and 3D-THRIVE sequences. Two radiologists independently evaluated the conventional axial 3D-FSE and CS-3D-FSE image sets on a picture archiving and communication system (PACS) workstation. The subscapularis, supraspinatus, and infraspinatus tendons were evaluated for the presence of lesions using a 4 point scale (0, normal; 1, tendinopathy; 2, partial-thickness tear; 3, full-thickness tear). The long-head of the biceps tendon was evaluated for the presence of lesions using a 3 point scale (0, normal; 1, tendinopathy; 2, tear). Two musculoskeletal radiologists (two board-certified fellowship-trained musculoskeletal radiologists with 6 and 2 years of subspecialty experience, respectively) independently and blindly assessed the randomized images.

Table 1. MR protocols of 3D-THRIVE without and with CS

Parameters	3D-THRIVE	CS-3D-THRIVE
Repetition time (ms)	7.2	7.2
Echo time (ms)	3.3	3.3
Matrix size	320 × 320	320 × 320
Field of view (mm)	160	160
Section thickness (mm)	1	1
Bandwidth (Hz/pixel)	289	289
Echo train length	80	80
NEX	1	1
SENSE factor	2 × 2	2 × 2
CS factor	-	1.5
Scan time (S)	104	81

MR, magnetic resonance; 3D-THRIVE, 3D-T1 high resolution isovolumetric examination; CS, compressed sensing; NEX, number of excitation; SENSE, sensitivity encoding.

In the second session, diagnostic agreements in the 3D-THRIVE sequence with and without CS were evaluated by two radiologists (two board-certified fellowship-trained musculoskeletal radiologists with 6 and 2 years of subspecialty experience, respectively) independently using the same scale. The axial THRIVE sequences and the reformatted sagittal and coronal images were reviewed by the reviewers.

The overall image quality and degree of artifacts were evaluated by a consensus. The overall image quality between conventional 3D-THRIVE without and with CS was evaluated using a 5 point scale (grade 5, excellent intersequence agreement on clarity of the anatomical structures of the shoulder; grade 4, good intersequence agreement on clarity of the anatomical structures; grade 3, acceptable intersequence agreement on clarity of the anatomical structures; grade 2, poor intersequence agreement on clarity of the anatomical structures; grade 1, no intersequence agreement on clarity of the anatomical structures), and the degree of artifacts was evaluated using a 4 point scale (grade 4, minimal or no motion artifact; grade 3, average motion artifact; grade 2, above average motion artifact; grade 1, unacceptable motion artifact). Diagnostic agreement for pathologic lesions of the supraspinatus, subscapularis, and biceps tendons between 3D-THRIVE with and without CS sequences was evaluated.

Statistical Analysis

3D-THRIVE diagnostic agreement for pathological shoulder tendon lesions between 2D FSE and 3D-THRIVE and between 3D-THRIVE with CS and 3D-THRIVE without CS sequences was evaluated using the intraclass correlation coefficient (ICC). The overall image quality scores and artifacts were compared between conventional 3D-THRIVE without CS and 3D-THRIVE with CS using a paired t-test. Inter-rater agreements were evaluated using a weighted kappa test.

RESULTS

The diagnostic agreements of 2D FSE and 3D-THRIVE for shoulder tendon pathologic findings showed excellent agreement in the supraspinatus, infraspinatus, subscapularis, and biceps tendons (Table 2, Fig. 2).

The scan time for isotropic 3D-THRIVE was reduced from 104 s without CS to 81 s with CS (Table 1). While the CS 3D-THRIVE images showed inferior image quality (4.466 ± 0.529 vs. 4.384 ± 0.520, $p = 0.033$) than 3D-THRIVE without CS, there were no significant differences in degree of artifacts between the two methods (3.822 ± 0.420 vs. 3.726 ± 0.507, $p = 0.090$). In comparison with 3D-THRIVE and CS-3D-THRIVE, the diagnostic agreement for pathologic findings showed excellent agreement with 3D-THRIVE without CS and CS in the supraspinatus, infraspinatus, subscapularis, and biceps tendons (Table 3, Fig. 3). Inter-rater agreements were good for the supraspinatus, infraspinatus, subscapularis, and biceps tendons (Table 4).

DISCUSSION

This study explored the application of CS to 3D gradient sequences, including 3D-THRIVE, for shoulder MRA. To assess the feasibility of conventional shoulder MRA with CS, this clinical study compared the imaging outcomes of conventional shoulder MRA with those of fast MRI with CS. The results demonstrated a reduction in scanning time by approximately 20%, from 104 s to 81 s, when utilizing CS MRA examination for shoulder patients without significant image quality degradation. Additionally, the isotropic nature of 3D gradient sequences, such as 3D-THRIVE, allows for high spatial resolution and volumetric scanning, facilitating MPR imaging akin to CT images, including oblique coronal, oblique sagittal, and axial planes, as well as radiologist-defined planes, without compromising im-

Table 2. Diagnostic agreement of 2D FSE and 3D-THRIVE for shoulder tendon pathology detection

	Reviewer 1	Reviewer 2
Subscapularis tendon	0.983 [0.972–0.989]	0.943 [0.909–0.964]
Supraspinatus tendon	0.982 [0.971–0.989]	0.988 [0.981–0.992]
Infraspinatus tendon	0.926 [0.881–0.953]	0.977 [0.963–0.985]
Long head of the biceps tendon	1.000	0.942 [0.907–0.963]

The data indicate the ICCs, with the lower and upper limits of the 95% confidence intervals in parentheses.
FSE, fast spin echo; 3D-THRIVE, 3D-T1 high resolution isovolumetric examination; ICC, intraclass correlation coefficient.

Table 3. Diagnostic agreement of 3D-THRIVE and CS-3D-THRIVE for shoulder tendon pathology detection

	Reviewer 1	Reviewer 2
Subscapularis tendon	1.000	1.000
Supraspinatus tendon	0.995 [0.992–0.997]	1.000
Infraspinatus tendon	0.927 [0.884–0.954]	1.000
Long head of the biceps tendon	1.000	1.000

The data indicate the ICCs, with the lower and upper limits of the 95% confidence intervals in parentheses.
3D-THRIVE, 3D-T1 high resolution isovolumetric examination; CS, compressed sensing; ICC, intraclass correlation coefficient.

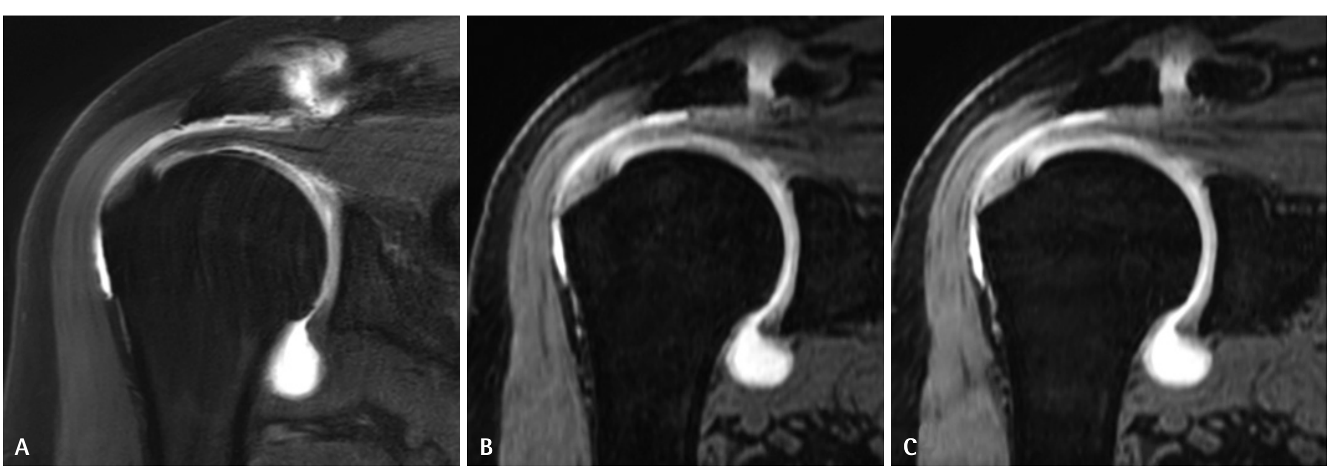

Fig. 2. Comparison of conventional 2D FSE T1-weighted images (A), conventional 3D-THRIVE (B) and 3D-THRIVE with CS (C). A: Conventional 2D FSE sequence requires longer examination time, making images are more vulnerable to motion artifacts, whereas 3D-THRIVE sequence with and without CS requires shorter examination time, resulting in decreased motion artifact. However, note the details on supraspinatus tendon attachment site and acromioclavicular joints are diminished in the THRIVE sequences (B and C). FSE, fast spin echo; 3D-THRIVE, 3D-T1 high resolution isovolumetric examination; CS, compressed sensing.

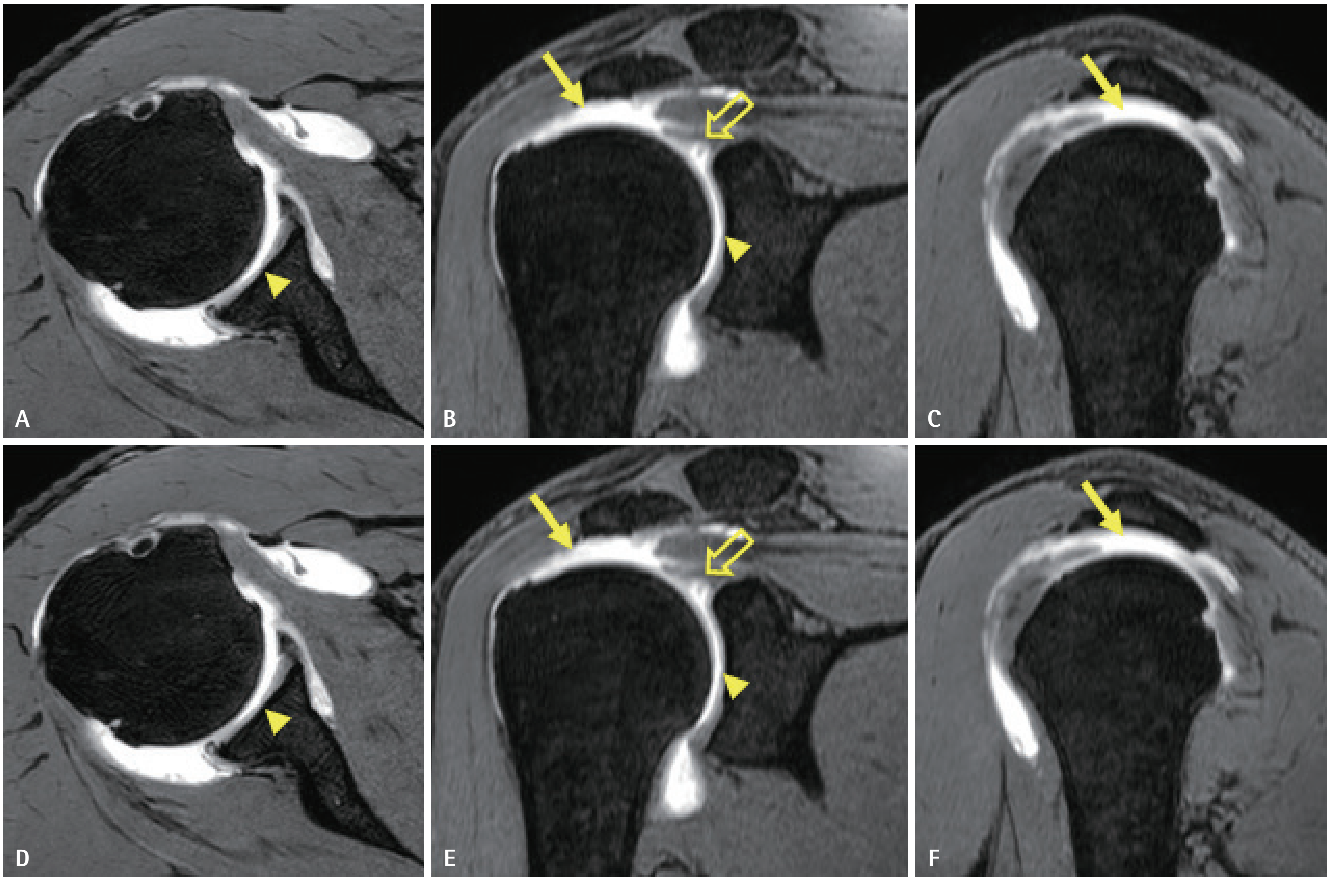

Fig. 3. A 53-year-old man with full-thickness supraspinatus tear. Axial, coronal, sagittal conventional 3D-THRIVE (A-C) and CS-3D-THRIVE shoulder MR images show full-thickness tear of supraspinatus tendon (arrows, C and F) (D-F), partial thickness cartilage defect less than 1 cm (arrowheads, A and D), superior labral tear (B and E). Two readers classified image quality as excellent (acceptable for diagnostic use), showing diagnostic radiologic findings as full-thickness tear of supraspinatus tendon, partial thickness cartilage defect less than 1 cm, superior labral tear on both conventional and CS-3D-THRIVE images. 3D-THRIVE, 3D-T1 high resolution isovolumetric examination; CS, compressed sensing; MR, magnetic resonance.

Table 4. Inter-rater agreements for shoulder tendon pathology detection

	2D FSE	3D-THRIVE	CS-3D-THRIVE
Subscapularis tendon	0.611 [0.439–0.783]	0.726 [0.586–0.866]	0.726 [0.586–0.866]
Supraspinatus tendon	0.684 [0.560–0.807]	0.729 [0.616–0.841]	0.748 [0.643–0.852]
Infraspinatus tendon	0.472 [0.229–0.716]	0.424 [0.173–0.674]	0.470 [0.222–0.718]
Long head of the biceps tendon	0.765 [0.619–0.911]	0.703 [0.531–0.875]	0.703 [0.531–0.875]

The data indicate weighted kappa values, with the lower and upper limits of the 95% confidence intervals in parentheses.
FSE, fast spin echo; 3D-THRIVE, 3D-T1 high resolution isovolumetric examination; CS, compressed sensing.

age quality.

The combination of CS application and isotropic acquisition enabled volumetric scanning of the shoulder joint in only 81 s. Isotropic 3D-THRIVE demonstrated image quality and diagnostic performance comparable to those of conventional 2D FSE sequences. As the MPR capability of CS-3D-THRIVE could be utilized instead of the three acquisitions of conventional 2D FSE/turbo spin echo sequences of oblique coronal, oblique sagittal, and axial planes, which usually take 5–7 min, it might be possible to implement ultrafast imaging by applying a combination of CS and isotropic acquisition.

Analyses were performed to investigate the diagnostic agreement of the pathological findings of the three anatomical lesions. First, for tendon lesions on the subscapularis, supraspinatus, infraspinatus, and biceps tendons, the CS 3D-THRIVE sequence showed almost identical diagnostic agreement to the image quality of 3D-THRIVE without CS. Second, while the CS 3D-THRIVE images showed inferior image quality, there were no significant differences in the degree of artifacts between the two sequences. The results showed that the differences between the CS and non-CS images did not affect the diagnostic agreement for the evaluation of shoulder pathology.

Our study had several limitations. First, the study results could be limited to MRI with direct arthrography, which consists of T1-weighted images with a relatively short relaxation time. However, CS was useful for all the MR sequences. Second, a comparison study with recently introduced deep learning reconstruction images was not performed. However, in the future, deep learning-reconstructed images will be compared with CS reconstruction images. The usefulness of deep learning reconstruction has been previously highlighted [19]; however, this study was conducted without deep learning reconstruction (DLR). Future research is required to evaluate the usefulness of DLR for fast imaging. Third, we acknowledge the potential selection bias owing to data exclusion. Future research should aim to mitigate these biases through a larger number of studies or prospective studies to ensure more robust and reliable results. Fourth, we did not evaluate labral pathology.

In conclusion, CS-accelerated isotropic 3D-THRIVE shoulder MRA produced images of of tendon pathology with acceptable diagnostic agreement and reduced scan time. However, a better imaging sequence is necessary for further evaluation of subscapularis tendinopathy.

Availability of Data and Material

The datasets generated or analyzed during the study are not publicly available due institution data protection policy but are available from the corresponding author on reasonable request.

Conflicts of Interest

The authors have no potential conflicts of interest to disclose.

Author Contributions

Conceptualization: Young Han Lee. Data curation: Jiwoo Park, Joohee Lee. Formal analysis: Jiwoo Park, Joohee Lee, Youngho Won. Funding acquisition: Young Han Lee. Methodology: Joohee Lee, Young Han Lee. Supervision: Young Han Lee, Ho-Taek Song. Writing—original draft: Youngho Won, Jiwoo Park, Joohee Lee. Writing—review & editing: Young Han Lee, Ho-Taek Song.

ORCID iDs

Youngho Won	https://orcid.org/0009-0006-4845-5882
Jiwoo Park	https://orcid.org/0009-0005-6048-2675
Joohee Lee	https://orcid.org/0000-0002-7721-8935
Ho-Taek Song	https://orcid.org/0000-0002-6655-2575
Young Han Lee	https://orcid.org/0000-0002-5602-391X

Funding Statement

This study was supported by a grant for the Korean Society of MSK MRI by the Korean Society of Magnetic Resonance in Medicine.

This work was supported by a National Research Foundation (NRF) grant funded by the Korean Government, Ministry of Science, and ICT (MSIP 2022R1F1A1071702).

Acknowledgments

None

REFERENCES

1. Magee T, Williams D. 3.0-T MRI of the supraspinatus tendon. AJR Am J Roentgenol 2006;187:881-886.
2. Magee TH, Williams D. Sensitivity and specificity in detection of labral tears with 3.0-T MRI of the shoulder. AJR Am J Roentgenol 2006;187:1448-1452.
3. Gusmer PB, Potter HG, Schatz JA, et al. Labral injuries: accuracy of detection with unenhanced MR imaging of the shoulder. Radiology 1996;200:519-524.
4. Alaia EF, Subhas N. Shoulder MR imaging and MR arthrography techniques: new advances. Magn Reson Imaging Clin N Am 2020;28:153-163.
5. Magee T. 3-T MRI of the shoulder: is MR arthrography necessary? AJR Am J Roentgenol 2009;192:86-92.
6. Blanchard TK, Bearcroft PW, Dixon AK, et al. Magnetic resonance imaging or arthrography of the shoulder: which do patients prefer? Br J Radiol 1997;70:786-790.
7. Saupe N, Zanetti M, Pfirrmann CW, Wels T, Schwenke C, Hodler J. Pain and other side effects after MR arthrography: prospective evaluation in 1085 patients. Radiology 2009;250:830-838.
8. Fox MG, Petrey WB, Alford B, Huynh BH, Patrie JT, Anderson MW. Shoulder MR arthrography: intraarticular anesthetic reduces periprocedural pain and major motion artifacts but does not decrease imaging time. Radiology 2012;262:576-583.
9. Jung JY, Yoon YC, Choi SH, Kwon JW, Yoo J, Choe BK. Three-dimensional isotropic shoulder MR arthrography: comparison with two-dimensional MR arthrography for the diagnosis of labral lesions at 3.0 T. Radiology 2009;250:498-505.
10. Lee SH, Yun SJ, Yoon Y. Diagnostic performance of shoulder magnetic resonance arthrography for labral tears having surgery as reference: comparison of high-resolution isotropic 3D sequence (THRIVE) with standard protocol. Radiol Med 2018;123:620-630.
11. Sodickson DK, Manning WJ. Simultaneous acquisition of spatial harmonics (SMASH): fast imaging with radiofrequency coil arrays. Magn Reson Med 1997;38:591-603.
12. Pruessmann KP, Weiger M, Scheidegger MB, Boesiger P. SENSE: sensitivity encoding for fast MRI. Magn Reson Med 1999;42:952-962.
13. Griswold MA, Jakob PM, Heidemann RM, et al. Generalized autocalibrating partially parallel acquisitions (GRAPPA). Magn Reson Med 2002;47:1202-1210.
14. Donoho DL. Compressed sensing. IEEE Trans Inf Theory 2006;52:1289-1306.
15. Lustig M, Donoho DL, Santos JM, Pauly JM. Compressed sensing MRI. IEEE Signal Process Mag 2008;25:72-82.
16. Lustig M, Donoho D, Pauly JM. Sparse MRI: the application of

compressed sensing for rapid MR imaging. Magn Reson Med 2007; 58:1182-1195.
17. Jaspan ON, Fleysher R, Lipton ML. Compressed sensing MRI: a review of the clinical literature. Br J Radiol 2015;88:20150487.
18. Lee SH, Lee YH, Song HT, Suh JS. Rapid acquisition of magnetic resonance imaging of the shoulder using three-dimensional fast spin echo sequence with compressed sensing. Magn Reson Imaging 2017;42:152-157.
19. Baek SD, Lee J, Kim S, Song HT, Lee YH. Artificial intelligence and deep learning in musculoskeletal magnetic resonance imaging. Investig Magn Reson Imaging 2023;27:67-74.